On the Impact of Non-Synchronous Devices over the Critical Clearing Time of Low-Inertia Systems

Julia R. Céu
University of São Paulo
São Carlos, Brazil
juliaceu14@usp.br

Guðrún M. Jónsdóttir
University College Dublin
Dublin, Ireland
gudrun.jonsdottir@ucdconnect.ie

Federico Milano
University College Dublin
Dublin, Ireland
federico.milano@ucd.ie

Rodrigo A. Ramos
University of São Paulo
São Carlos, Brazil
rodrigo.ramos@ieee.org

***Abstract*—This paper discusses the impact of the inertia of conventional power plants as well as of the frequency control of non-synchronous devices on the Critical Clearing Time (CCT) following a three-phase fault in a benchmark power system model. The non-synchronous devices studied in this paper are wind power plants, energy storage devices, and an average model of thermostatically controlled loads. The case study consists in a parametric analysis where the total inertia of the system is varied and the dynamic response of the system is evaluated by considering different scenarios and control strategies. Simulation results lead to the non-intuitive conclusion that, for any given level of inertia, non-synchronous devices always lead to an increase in the CCT of the system.**

***Index Terms*—Transient stability, critical clearing time (CCT), non-synchronous generation, energy storage systems (ESS), thermostatically controlled load (TCL).**

I. Introduction

Power systems all around the world are currently facing several open challenges, e.g., environmental concerns and difficulties related to the connection of devices based on new technologies. There is a strong incentive for the use of alternative energy sources interfaced by electronic power devices to generate electrical energy in large-scale systems. As opposed to synchronous machines, non-synchronous devices usually have very limited frequency regulation capability [1], which may have an impact on the stability of the system [2].

Recent publications, such as [3] or [4], for example, show that low levels of rotational inertia have a great impact on power system stability and operation. As stated in [4], high shares of Renewable Energy Sources (RESs), such as wind turbines, can be treated as a reduction of the rotational inertia in power systems. In other words, the inception of these power sources causes reduction of frequency support, mainly because RESs are connected to the grid through power electronics devices. This type of connection creates a partial decoupling of the dynamics of the primary energy source from the ones of the electrical grid, making these sources less sensitive to the Rate of Change of Frequency (RoCoF).

Non-synchronous devices only react to frequency variations when a specific designed control exists. For this reason, the authors in [5], [6] test the effectiveness, in terms of system reliability and stability, of droop-type and RoCoF-based controllers of wind power plant and enesrgy storage systems (ESSs). The droop portion may be compared to primary frequency controllers of synchronous machines, and has a remarkable efficiency in mitigating the frequency nadir, although it does not respond as fast as the RoCoF portion, which operates faster due to its sensitivity to the rate of change of frequency [5]. On the other hand, the effectiveness of non-synchronous devices to improve the transient stability margin of power systems has been shown to be limited [7].

Another class of non-synchronous devices able to provide frequency support are felixble loads. And among these, Thermostatically Controlled Loads (TCLs) are consisdered in this paper. Although these types of loads are usually scattered throughout the system, an average model [8], [9] is often used to describe the aggregate effect of TCL on the CCT in a power system. As will be seen later, the results of the analyses reinforces the main point that the reduction of the equivalent inertia is not always the key factor to explain the behavior of the system. The same conclusion can be taken from a number of experiments with energy storage devices, modeled as in [10] presented in this paper.

It is a common understanding that non-synchronous DERs lowers the CCT of a grid. This happens because introducing DERs is generally achieved by reducing the amount of conventional generation and, hence, the inertia available in the system. However the reduction of inertia and commitment of DERs do not need to come together. The objective of this paper is to evaluate the impact of non-synchronous devices on the CCT after the occurrence of a fault for given amounts of inertia. Simulation results show that DERs per se do not necessarily worsen the CCT but can actually contribute to it, especially (but not necessarily) if they provide some frequency control.

The paper is organized as follows. Section II presents the

This work was supported by FAPESP through funding J. R. Céu and R. A. Ramos under Grants No. 2018/25853-0 and 2019/11703-9, respectively, and by the Science Foundation Ireland by funding J. R. Céu, G. Jónsdóttir and F. Milano under project AMPSAS, Investigator Programme, Grant No. SFI/15/IA/3074.

978-1-7281-7455-6/20/$31.00 ©2020 IEEE

device models used in this study. This section describes how each type of device is connected to the system and describes the hypotheses about their behavior. Section III explains how the simulation of each case was performed and the respective obtained results. A detailed explanation on the mechanism used to insert the RES and how it affects the system equivalent inertia is provided. Conclusions are given in Section IV.

II. Modelling

This section outlines the models considered in the case studies. Constant impedance load models were assumed for scenarios except for those involving TCLs.

A. Swing Equation

Any study about the effect of inertia on the behavior of a synchronous machine can start from very basic concepts related to the well-known swing equations [2]:

$$M\,\dot{\omega} = p_{\mathrm{m}} - p_{\mathrm{e}} - D\,\omega\,, \tag{1}$$

where:

- ω: angular frequency
- M: inertia constant
- D: damping constant
- p_{m}: mechanical power
- p_{e}: electrical power

A key assumption of this paper is the way in which the total system inertia is calculated. Based on the concept of equivalent inertia and taking (1) into account, the total equivalent inertia of the system is considered to be the algebraic sum of all individual inertia constants of the generators [4].

B. Wind Power Plants

Modeling of wind power plants is a topic that is widely studied by the power systems community and there are several models available in the literature ([11] and [12] are examples). There are differences among the models but the vast majority of them is related to the control objective of the converters (e.g., [13]–[16]).

In this paper, the wind generator model used consists of a 5$^{\text{th}}$ order doubly-fed induction generator model driven by a turbine which adopts a constant wind speed model. This is a built-in model available in the software used to perform the simulations [17].

As previously stated, resources which are connected to the grid via power electronics devices are able to provide very little (if any) frequency support to the system when compared to synchronous generators [1]. According to (1), the higher the inertia constant is, the lower frequency deviations are. Wind turbines normally do not provide any extra rotational inertia to the system. Thus, the equivalent system inertia is low for power systems with high shares of wind turbines. In this case frequency dynamics become faster, which might make traditional solutions to minimize frequency deviations too slow [1].

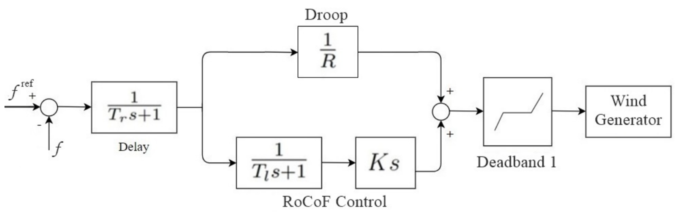

Fig. 1. Block scheme for droop and RoCoF control.

The wind generators can provide frequency support by including wind turbine frequency control. A common approach for wind turbine frequency control is to bypass the Maximum Power Point Tracking (MPPT) and set the power output based on the deviation of the measured frequency (droop control) and/or Rate of Change of Frequency (RoCcF) control. A combination of these two ,as presented in [5] is shown in Fig. 1. The droop controller is related to the primary frequency control of the system, while the RoCoF controller produces the virtual inertial response. Thus, the latter one is more likely to have an impact on the CCT of the system since it has a faster control action.

C. Energy Storage Systems

In this paper the simplified Energy Storage System (ESS) model shown in Fig. 2 [10] is utilized. The ESS is represented through decoupled active and reactive power controllers. The input signal ω is the frequency of the Center of Inertia (COI) that is regulated by the (active) power balance of the system. The assumption that this signal is easily available for implementation may not hold in practice, so replacing this model with another one in which the input signal is a local frequency is among the future perspectives of this work. The voltage at the point of connection v_{ac} is regulated through the ESS reactive power. The physical behavior of the storage system is synthesized by two lag blocks with time constants $T_{P,\mathrm{ESS}}$ and $T_{Q,\mathrm{ESS}}$, which are both equal to 2.6 ms in all studied cases.

1) Thermostatically Controlled Loads: Thermostatic controllers regulate the frequency by varying the load active power consumption through a variation of the load reference temperature (see Fig. 3). These controllers are coupled directly to system loads, in such a way that they represent (together with the lumped load model to which they are connected) an average model of several TCLs scattered across the low and medium voltage subsystems. The temperature can vary a few degrees without affecting the behavior of the load and this allows a certain flexibility in the load demand. The frequency gain value assumed is 100, and the thermal time constant is $T_{Th,\mathrm{TCL}} = 500$ s.

The wind power plant and ESS models presented in this section also include a voltage control capability. This ability to provide reactive power support is due to the power electronic converter with which these devices are

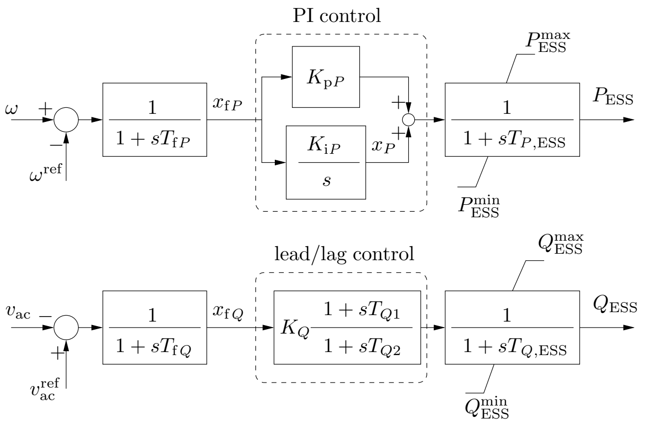

Fig. 2. Block diagram of the simplified ESS model used in the case studies.

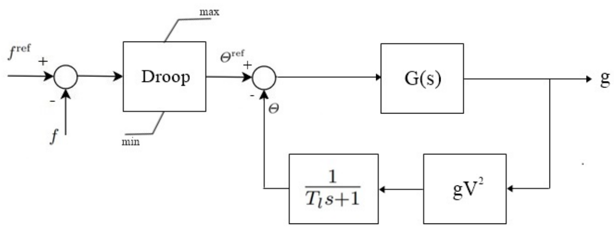

Fig. 3. Block diagram of thermostatically controlled loads used in the case studies.

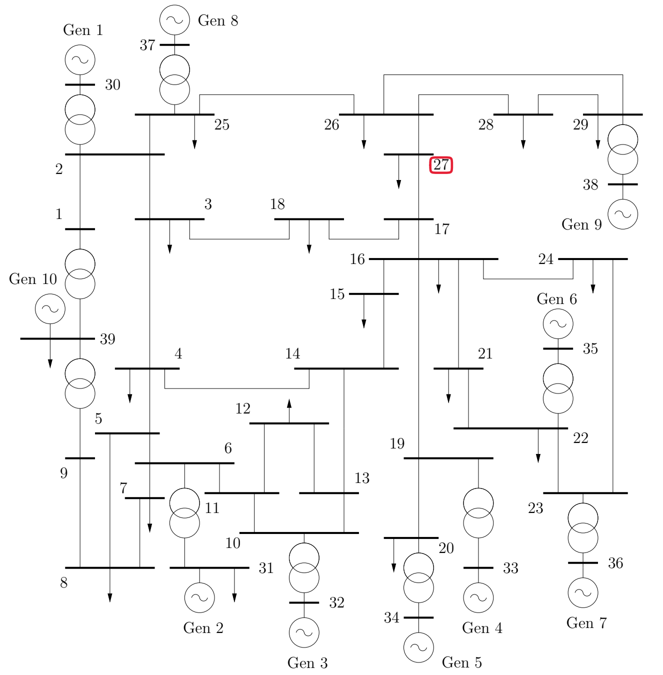

Fig. 4. Scheme of the New England 39-bus 10-machine system [18].

TABLE I
Inertia Constants of the Synchronous Generators of the New England System

Generator #	Inertia [s MW/MVA]	Generator #	Inertia [s MW/MVA]
1	1000	6	69.6
2	60.6	7	52.8
3	71.6	8	48.6
4	57.2	9	69.0
5	52.0	10	84.0

equipped. Although this extra reactive power support is small compared to that provided by synchronous generators, it plays a relevant role in the dynamics of interest in this paper, as shown in the following sections.

III. Case Study

The test system used in this case study is the benchmark IEEE 39-bus 10-machine New England system shown in Fig. 4. The network consists of 39 buses, 9 generators and one equivalent generator that represents the New York system to which the New England system is interconnect. The reference frequency is 50 Hz. The values for the inertia constants of each of the synchronous generators are presented in Table I. Further details on the system model are provided in [18]. All simulations presented in this case study were carried out using Dome a Python-based software tool for power system analysis [17]. The contingency for all transient stability analysis in this case study is a three-phase fault at bus 27, highlighted in Fig. 4.

In this case study the effect of changing the total inertia of the system on the systems Critical Clearing Time (CCT) is studied. This is done by modifying the test system in the following two ways.

- **Method I:** The inertia of each of the synchronous generators in the system is varied independently (Subsection III-A).
- **Method II:** Wind generation is installed at a factious bus next to all the synchronous generator buses, except Generator 1. The inertia of each synchronous generator is then varied independently and its generated power lowered proportionally. This power is in this case supplied by the equivalent wind generators so that the net generation of the system does not change (Subsection III-B-III-D).

A simple bisection algorithm is applied for each interaction in order to find the corresponding CCT for each inertia scenario. This technique is able to find the CCT value performing a repeated bisection of sub-intervals [19]. The numerical tolerance is of four decimals, computing the rounded result with three decimals. Then, a Python-based script was implemented that varies, according to a normally random percentage. The inertia in both cases is varied between $50-99\%$ of the test systems original inertia values. The CCT for each scenario is found by launching Dome at each iteration of the bisection algorithm. For each scenario discussed in this section, 5.000 inertia value scenarios were considered.

A. Original System

For this initial scenario, simulations of the original version of the New England system are carried out and the inertia is varied using Method I. Thus, in this case, only synchronous generators are present in the system. The results obtained for this case are utilized as a reference for the remaining scenarios. Figure 5 shows the values of the CCT for the original case scenario.

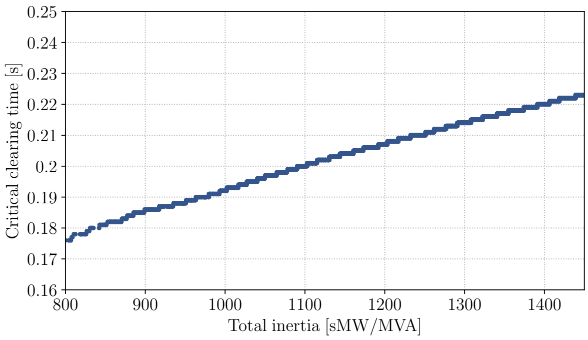

Fig. 5. The CCT values when varying the total equivalent inertia of the original New-England system.

The swing equation (1) suggests that larger values of the total equivalent inertia lead to a larger CCT. This inference is confirmed by the results shown in Figure 5. The CCT results range from approximately 0.17 s to approximately 0.23 s in Fig. 5.

B. Wind Power Plants

In this case the wind power plants are installed in the system alongside the synchronous generators and the inertia is varied using Method II. Two scenarios involving wind power plants are considered in this case: without and with their respective frequency controllers activated. Wind power plants are connected to the same buses as synchronous machines 2 to 10 through a transmission line. Figure 6 shows the results obtained for this modified system with wind power plants with and without frequency control.

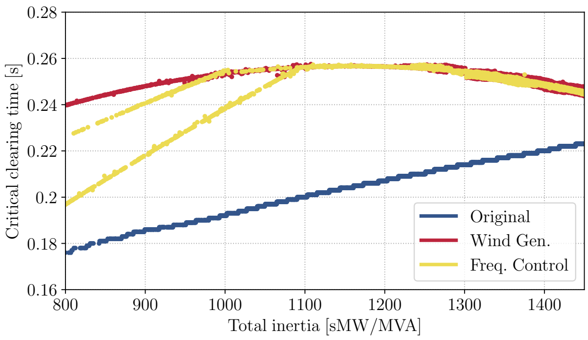

Fig. 6. The CCT values when varying the equivalent inertia of the New-England system including wind turbines with and without frequency control.

The results displayed in Figure 6 contradict simple inferences that can be drawn from the swing equation (1). First, the inclusion of wind turbines increases the CCT for any given value of inertia. This is due to the fact the wind power plants are non-synchronous and thus do not increase their kinetic energy (and, thus, do not contribute accelerating the rotor of synchronous machines) during the fault as synchronous machine do. This explains also why, when the system has lower equivalent inertia (i.e., in the case where the frequency controllers of the wind generators are not active), the obtained CCTs are relatively higher with respect to the base case than for high values of the inertia.

Less intuitive is the effect of the frequency control of wind power plants. In this case, the behavior of the system is more complex as the frequency control impacts differently and unpredictably depending on the inertia, controller limits and the wind generation level.

C. Energy Storage Systems

In this case the inertia is varied using Method II, thus with wind installed in the system. Figure 7 shows the CCT behavior when ESSs are added to the original New England system. Two scenarios are considered, namely with one or two ESSs. In the first scenario, the ESS is located at bus 16. In the second scenario, the ESSs are connected to buses 7 and 16.

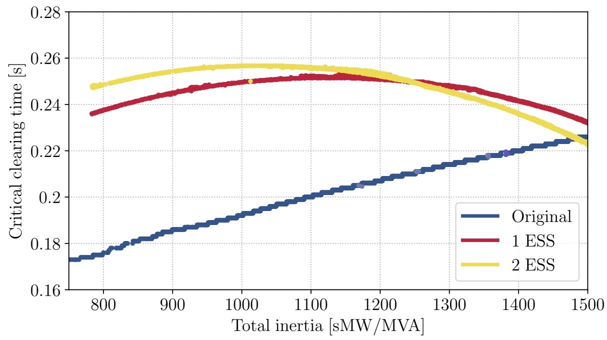

Fig. 7. The CCT values when varying the equivalent inertia of the New-England system including ESSs.

The frequency and voltage control capability of ESSs is assumed to be bigger than that of wind power plants, and hence ESSs should increase the CCT compared to the case with only wind. This is confirmed in the conclusions given in [7]. Figure 7 shows that including one ESS gives almost identical results to the case with wind without frequency control, as presented in Fig. 6. Adding the second ESS does increase the CCT for lower inertia values.

The results shown in Fig. 7 indicate that simple inferences based solely on the swing equation of the system must be carefully tested. In this case, in fact, the voltage control provided by the ESSs is the dominant factor that impact on the CCT of the system.

D. Thermostatically Controlled Loads

In this last scenario, the New England system is modified by including TCLs with frequency support at all load buses. Wind generators without frequency controllers were preserved in this case and, therefore, the modified system consists of 10 synchronous machines, 9 wind generators and 19 TCLs (one for each aggregate load model in the system). The inertia is varied using Method II and the results are shown in in Fig. 8.

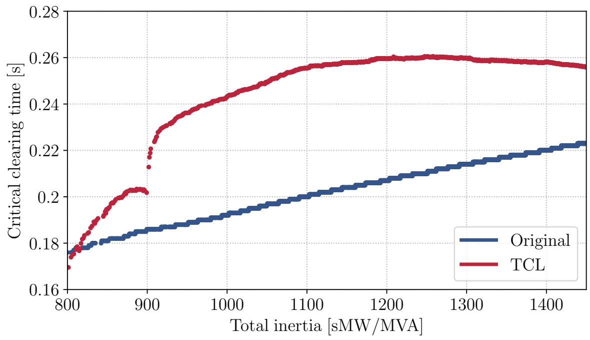

Fig. 8. The CCT values when varying the equivalent inertia of the New-England test system with wind turbines without frequency control and TCLs.

Including the TCLs does result in increased CCTs for higher inertia values. On the other hand for inertia values lower than approximately 950 the CCT drops drastically and for inertia values lower than about 800 the CCTs are lower than for the original case.

As in the scenario with wind power plants with frequency control, there is no simple explanation for the observed behavior since there are several factors interacting to produce the observed results. TCLs are relatively slow devices and so is their frequency control, much slower than the time scale of the inertial response of synchronous machines and their loss of synchronism. This could explain the behavior seen in Fig. 8. That is for lower inertia values the TCLs does not improve the CCTs.

IV. Conclusion

The paper presents a transient stability analysis of four different scenarios of the IEEE New England power system. These consist of coupling wind power plants, ESSs and TCLs with frequency support. The case study show some counterintuitive results that cannot be directly inferred from classical swing equation of synchronous machines. The main conclusion is that the total equivalent inertia of the system is not necessarily the only factor that determines the CCT of the system. In most of the presented results, the extra amount of voltage regulation provided by the power electronic converters of wind power plants and ESSs appears to be a significant effect, even higher than the frequency support provided by the same devices.

It is important to remark that this is a preliminary study that precedes a more in-depth analysis of the analyzed phenomena. However, the presented case study already provides interesting insights. Future work will involve the application of more realistic models (particularly for the ESS) and a careful analysis of the properties of the stability region for all studied cases.

References

[1] F. Milano, F. Dörfler, G. Hug, D. J. Hill, and G. Verbič, "Foundations and challenges of low-inertia systems," in *Power Systems Computation Conference (PSCC)*, Dublin, Ireland, 2018, pp. 1–25.

[2] P. Kundur, *Power system stability and control.* McGraw-hill New York, 1994, vol. 7.

[3] H. Karbouj, Z. H. Rather, D. Flynn, and H. W. Qazi, "Non-synchronous fast frequency reserves in renewable energy integrated power systems: A critical review," *International Journal of Electrical Power and Energy Systems*, vol. 106, pp. 488 – 501, 2019.

[4] A. Ulbig, T. S. Borsche, and G. Andersson, "Impact of low rotational inertia on power system stability and operation," *IFAC Proceedings Volumes*, vol. 47, no. 3, pp. 7290–7297, 2014.

[5] J. Cerqueira, F. Bruzzone, C. Castro, S. Massucco, and F. Milano, "Comparison of the dynamic response of wind turbine primary frequency controllers," in *IEEE PES General Meeting*, Chicago, IL, 2017, pp. 1–5.

[6] Á. Ortega and F. Milano, "Modeling, simulation, and comparison of control techniques for energy storage systems," *IEEE Transactions on Power Systems*, vol. 32, no. 3, pp. 2445–2454, 2017.

[7] ——, "Stochastic transient stability analysis of transmission systems with inclusion of energy storage devices," *IEEE Transactions on Power Systems*, vol. 33, no. 1, pp. 1077–1079, 2018.

[8] S. Kundu, N. Sinitsyn, S. Backhaus, and I. Hiskens, "Modeling and control of thermostatically controlled loads," *arXiv preprint arXiv:1101.2157*, 2011.

[9] F. Milano, *Power system modelling and scripting.* Springer Science & Business Media, 2010.

[10] Á. Ortega and F. Milano, "Generalized model of VSC-based energy storage systems for transient stability analysis," *IEEE Transactions on Power Systems*, vol. 31, no. 5, pp. 3369–3380, 2015.

[11] J. G. Slootweg, S. W. H. de Haan, H. Polinder, and W. L. Kling, "General model for representing variable speed wind turbines in power system dynamics simulations," *IEEE Transactions on Power Systems*, vol. 18, no. 1, pp. 144–151, Feb 2003.

[12] G. Abad, J. Lopez Taberna, M. A. Rodríguez, L. Marroyo, and G. Iwanski, *Doubly Fed Induction Machine: Modeling and Control for Wind Energy Generation.* John Wiley & Sons, September 2011, vol. 86.

[13] M. Kayikci and J. V. Milanovic, "Dynamic contribution of DFIG-based wind plants to system frequency disturbances," *IEEE Transactions on Power Systems*, vol. 24, no. 2, pp. 859–867, May 2009.

[14] G. Ramtharan, J. B. Ekanayake, and N. Jenkins, "Frequency support from doubly fed induction generator wind turbines," *IET Renewable Power Generation*, vol. 1, no. 1, pp. 3–9, March 2007.

[15] L. A. G. Gomez, B. G. Bueno, A. P. Grilo, A. J. S. Filho, and M. Salles, "Analysis of the doubly fed induction generator performance on frequency support of microgrids," in *2017 North American Power Symposium (NAPS)*, Sept 2017, pp. 1–6.

[16] D. Ochoa and S. Martinez, "Fast-frequency response provided by dfig-wind turbines and its impact on the grid," *IEEE Transactions on Power Systems*, vol. 32, no. 5, pp. 4002–4011, Sep. 2017.

[17] F. Milano, "A Python-based software tool for power system analysis," in *IEEE PES General Meeting*, Vancouver, BC, 2013.

[18] C. Cañizares, T. Fernandes, E. Geraldi Jr, L. Gérin-Lajoie, M. Gibbard, I. Hiskens, J. Kersulis, R. Kuiava, L. Lima, F. Marco, N. Martins, B. Pal, A. Piardi, R. Ramos, J. Santos, D. Silva, A. Singh, B. Tamimi, and D. Vowles, "Benchmark systems for small signal stability analysis and control," *IEEE Transactions on Power Systems*, vol. 32, no. 1, pp. 715–722, 2017.

[19] R. L. Burden and J. D. Faires, *Numerical Analysis.* Cengage Learning, 2010.